GT2008-50658

AN INNOVATIVE GAS TURBINE CYCLE
WITH METHANOL FUELLED CHEMICAL-LOOPING COMBUSTION

Hongguang Jin[1]*, Xiaosong Zhang[1,2], Hui Hong[1], Wei Han[1]

[1]Institute of Engineering Thermophysics, Chinese Academy of sciences, Beijing 100080, China
Tel: 86-10-82543032   Fax: 86-10-82622854   E-mail. hgjin@mail.etp.ac.cn
[2]Graduate University of the Chinese Academy of Sciences

ABSTRACT

In this paper, a novel gas turbine cycle integrating methanol decomposition and the chemical-looping combustion (CLC) is proposed. The system study on two methanol-fuelled power plants, the new gas turbine cycle with CLC combustion, and a chemically intercooled gas turbine cycle, has been investigated with the aid of the exergy analysis (EUD methodology). In the proposed system, methanol fuel is decomposed into syngas mainly containing H_2 and CO by recovering low-temperature thermal energy from an intercooler of the air compressor. After the decomposition of methanol, the resulting product of syngas is divided into two parts: the most part reacting with Fe_2O_3, is sent into the CLC subsystem, and the other part is introduced into a supplement combustor to enhance the inlet temperatures of turbine to 1100-1500°C. As a result, the new methanol-fuelled gas turbine cycle with CLC had a breakthrough in performance, with at least about 10.7 percentage points higher efficiency compared to the chemically intercooled gas turbine cycle with recovery of CO_2 and is environmentally superior due to the recovery of CO_2. This new system can achieve 60.6% net thermal efficiency with CO_2 separation. The promising results obtained here indicated that this novel gas turbine cycle with methanol-fuelled chemical looping combustion could provide a promising approach of both effective use of alternative fuel and recovering low-grade waste heat, and offer a technical probability for CLC in applying into the advanced gas turbine with high temperatures above 1300°C.

INTRODUCTION

Currently, we face a potentially serious problem of rapid climate change due to anthropogenic emissions of greenhouse gases (e.g. CO_2). One of the options to control the greenhouse gas emission is the CO_2 capture technologies from flue gases. In a fossil fuel-fired power plant, CO_2 capture can be carried out mainly through three available technologies: "pre-combustion," "post-combustion" and "oxy-fuel combustion." The progress in this field has been addressed by Mazen [1]. The main disadvantage of these techniques is both the substantial addition to the cost of power generation and the large amount of energy that is required for the separation of CO_2, which means a relative reduction in the overall efficiency of a power plant of 15-20% [2][3]. It is important and urgent to find a new method where CO_2 can be separated from the flue gases in the power plant with a small decrease in efficiency.

Chemical-looping combustion (CLC) with inherent separation of CO_2 is considered a promising technology proposed by Ishida and Jin in 1994 [4][5]. It is the most attractive energy efficient method for CO_2 capture from fuel conversion in combustion process. Compared to conventional combustion, the chemical-looping combustion involves the use of a metal oxide as an oxygen carrier, which transfers oxygen from the combustion air to the fuel, and the direct contact between fuel and combustion air is avoided. In this way, CO_2 and H_2O are inherently separated from the other components of flue gases leading to no energy needed for CO_2 separation. It is worthy emphasized that this novel CO_2 capture technology simultaneously resolve both energy and environmental problems in a combustion processes, since the conversion of fuel-based chemical energy into chemical energy in the

Copyright © 2008 by ASME

traditional combustion not only results in the largest irreversibility in power system, but also gives rise to a seriously environmental impact. In recent years, several researchers have investigated and contributed in the development of the chemical looping combustion technology [6][7]. For example, Lyngfelt and his research group have designed and proposed a 10kW fluidized-bed boiler with chemical looping combustion [8], and Korea [9] has developed a 50kW chemical looping combustor for the future industrial application. A project for a novel CO_2 separation system with CLC has been conducted by the Department of Energy of the United States [10].

In our previous paper [4][11][12], Jin has creatively integrated and proposed three kinds of gas turbine thermal cycles coupling different fuels of natural gas, hydrogen and coal gas with chemical looping combustion, respectively. The kinetics catalysis and reaction for various kinds of fuelled-based chemical looping combustions have also been investigated [13][14]. With the development of alternative fuels such as methanol or DME, there is a great potential application in the power generation sectors. Especially for China and USA where coal is the main energy resource, methanol or DME (dimethylether) is economically produced from the promising coal based polygeneration technology (POLYGEN). However, when alternative fuel being converted into thermal energy for generating electricity by traditional combustion in the conventional power plant, we have to face a serious issue that there are yet both the largest exergy destruction of chemical energy and the high energy penalty for CO_2 due to containing carbon. Hence, one of the biggest potential for the development of the next-generation power plant using alternative fuel would be directed toward to the new approach of the fuel conversion. The chemical-looping combustion can be the promising candidate. In the present paper, the new fuel conversion method of chemical looping combustion is applied into the methanol fuelled intercooling gas turbine cycle.

The objective of this paper is (i) to propose a new methanol-fuelled combined cycle synergistically integrating chemical-looping combustion; (ii) to identify the characteristics of the new system with the aid of the graphical exergy methodology; (iii) and to disclose the potentials for reducing the energy penalty of CO_2 separation.

NOMENCLATURE

CC	Combined Cycle
CLC	Chemical-Looping Combustion
TIT	Turbine inlet temperature (^{o}C)
π	Pressure ratio
η	Thermal efficiency (LHV)
ΔE	Exergy change (kJ/mol)
ΔH	Enthalpy change (kJ/mol)
A	Energy level

SUBSCRIPTS

opt	optimal value
ed	energy donor
ea	energy acceptor
ox	oxidation reaction
re	reduction reaction
comp	compressor
GT	gas turbine
ST	steam turbine

DESCRIPTION OF THE TWO METHANOL-FUELLED POWER SYSTEMS

Methanol-fuelled power plants with CLC

Figure 1 shows the plant scheme of the new system. The plant includes three main parts: the methanol decomposition subsystem with the recovery of the low-grade waste thermal energy, the CLC subsystem fired by the syngas and the CO_2 separation subsystem.

Methanol decomposition subsystem Since in the conventional intercooled gas turbine, the heat at around 200-300ºC is wasted, methanol decomposition can be utilized to recover the intercooling heat. The compressed air (stream 1) with low pressure is cooled down to 130ºC in an intercooler, and is then compressed in the next stage compressor (stream 2) in the methanol decomposition subsystem. The intercooler heat is recovered through methanol decomposition. The intercooler is divided into two segments containing a heat exchanger and a reactor. The liquid methanol as a fuel, at the pressure of 15 bar, is first superheated to methanol vapor at the temperature of 220ºC. After that, the superheated methanol then proceeds to an endothermic reaction with catalyst in the reactor (stream 3). The endothermic reaction path is $CH_3OH \rightarrow CO+2H_2$ and absorbs the thermal energy of 96kJ/mol–CH_3OH at 220ºC, after which the syngas then enters the CLC subsystem. Because of the using of intercooling, the heat recover should be adopted.

CLC subsystem In the CLC subsystem, two separate reactors, syngas with metal oxide (reduction) and the resulting metal with air (oxidation), are used. Here the particle of Fe_2O_3 is used as a solid metal oxide (i.e. looping material) in the chemical-looping combustion. Oxygen is transferred between the two reactors by means of an oxygen carrier. The syngas is first reacted with the solid Fe_2O_3 as shown in reaction (1) in a reduction reactor,, producing solid FeO and steam. When 95%

Copyright © 2008 by ASME

of Fe_2O_3 is reduced, the equilibrium temperature reaction (1) is about 360 °C. To achieve a higher conversion ratio of Fe_2O_3, the temperature of the reduction reaction is set at 425°C. In the oxidation reactor, the air is reacted with the solid FeO as shown in reaction (2) in high-temperature produced from the former reactor yielding Fe_2O_3 and high-temperature flue gas through strong exothermic oxidation.

temperature is about 120°C, 15bar from the HRSG, before it is cooled down to 30°C by the condenser. At this temperature, the H_2O turns into its liquid form and the CO_2 is separated at 15bar.

Reference system In the previous paper [15], we have proposed a methanol-fuelled chemically intercooling gas turbine plant with the integration of low–temperature thermal
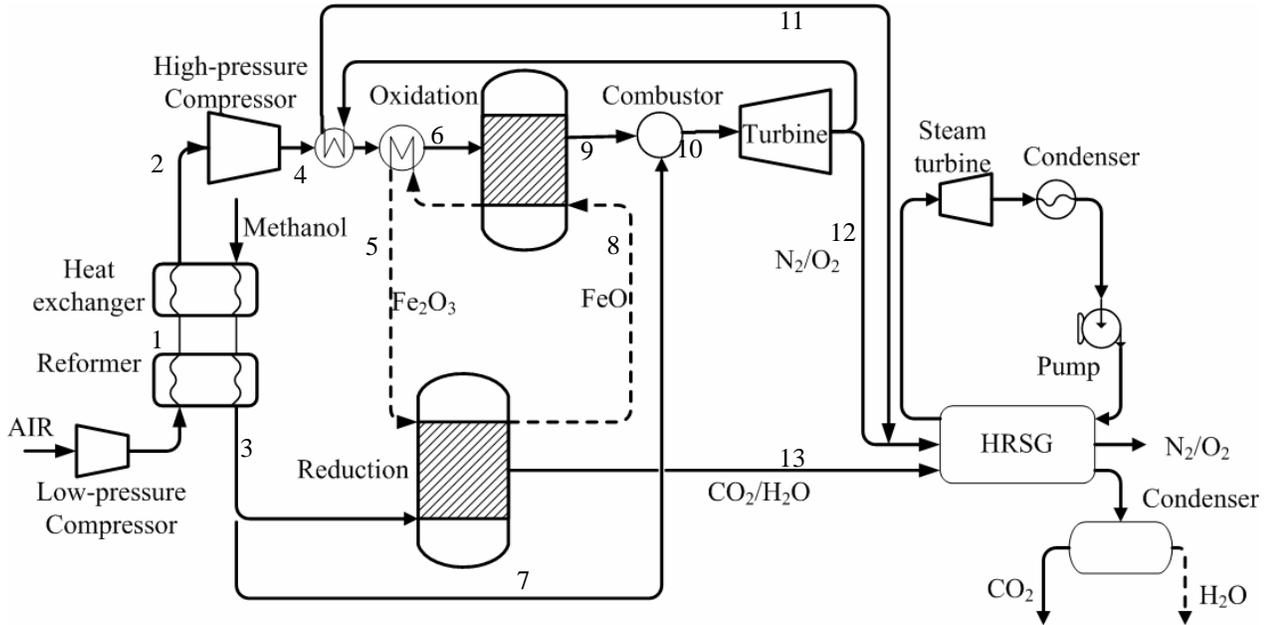
Figure 1 The flow diagram of the new system

Supplementary combustor subsystem Due to the physical characteristics of FeO, the temperature of oxidation cannot, however be higher than 1000°C [7]. To reach a higher gas turbine inlet temperature (TIT), a supplementary combustor is adopted. Most of the syngas enters the oxidation reactor, and the rest as fuel is fed into the supplementary combustor after the exiting of the oxidation reactor in order to enhance the inlet temperature of gas turbine ranging 1100-1500°C. Finally, the gases from the oxidation and reduction reactors can be used as the working fluid to generate power in the turbines. Then part of flue gas (stream 11) is drawn out to heat the compressed air and then go back to the dual-pressure HRSG as a heat resource with the other part flue gas.

Reduction:

$$3Fe_2O_3 + CO + 2H_2 \longrightarrow 6FeO + CO_2 + 2H_2O,$$

$$\Delta H^0_{Red} = 80kJ \qquad \text{Reaction (1)}$$

Oxidation:

$$6FeO + 3/2O_2 \longrightarrow 3Fe_2O_3,$$

$$\Delta H^0_{Oxd} = -840kJ \qquad \text{Reaction (2)}$$
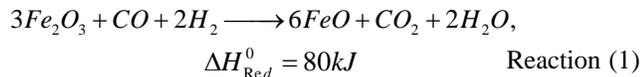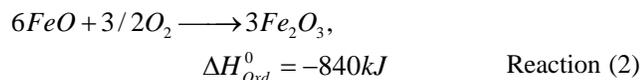
CO_2 separation The CO_2 separation subsystem is used to separate CO_2 from the mixture of CO_2/H_2O. The mixture's

energy and methanol decomposition. Figure 2 shows the flow diagram of the reference system.
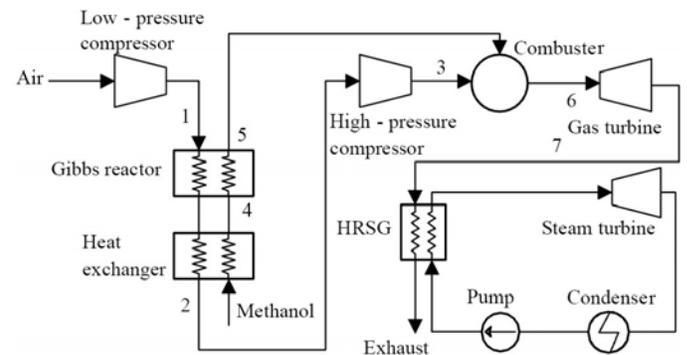
Figure 2 A simplified diagram for the chemically intercooled gas turbine combined cycle

The liquid fuel methanol, at the pressure of 15bar, is first superheated to methanol vapor at the temperature of 220°C. After that, the superheated methanol proceeds to an endothermic reaction with catalyst in the reactor and is

3 Copyright © 2008 by ASME

decomposed by the intercooler heat. The syngas fuel with primary H_2 and CO (stream 5) is fed to a combustor of the gas turbine and burned with the compressed air (stream 3). This exothermic reaction is according to $CO+2H_2+1.5O_2 \rightarrow CO_2+2H_2O$ and its heating value of combustion is 772.29kJ/mol–CH_3OH. The flue gas leaving the combustor (stream 6) is expanded in a gas turbine with the inlet temperature of 1300ºC. Exhaust gas from gas turbine of 500ºC–600ºC (stream 7) then drives a steam turbine through dual-pressure heat recovery steam generator (HRSG).

EVALUATION OF THE SYSTEM PERFORMANCE

This paper presents an evaluation of the system performance with ASPEN PLUS software. The pressure in the reactors was 15bar, and the exhaust gas temperature was 120ºC. The cooling air fraction is specified for each cooled stage and the value of the cooling air fraction is about 7 percent of the air compressor inlet flow. The temperature of water and CO_2 existing in the condenser was 25ºC, 15bar. The data of unit operation is specified in Table 1.

Table 1 Main assumption for evaluation

	Reference system	New system
Turbine inlet temperature, ºC	1300	1300
Turbine inlet pressure, bar	15.00	15.00
Reduction temperature, ºC	-	425
Pressure of the reduction reactor, bar	-	15.00
Pressure loss of heat exchangers, %	3.00	3.00
Isentropic efficiency of air compressor	0.88	0.88
Isentropic efficiency of gas turbine	0.90	0.90
Isentropic efficiency of steam turbine	0.88	0.88
Pinch point in HRSG, ºC	15	15
Pressure loss of HRSG (gas-side), %	3	3
Pressure loss of HRSG (steam, water),%	10	10
Condensation pressure, bar	0.07	0.07

Based on the analysis of the system model, this system has four important variables: (i) the turbine inlet temperature (TIT) of the high-temperature gas turbine; (ii) the total pressure ratio (π) of the compressor; (iii) the temperature (T_{re}) of the reduction reactor; (iv) the pressure ratio (π_1) of low-pressure compressor.

For a given case of the new system, four variables, TIT, π, T_2 and π_1, were set at 1300ºC, 15.00, 425ºC and 7.92, respectively. As a result, the thermal efficiency of the system is expected to be 60.6% with a CO_2 recovery ratio of 70%.

Table 2 Parameters of main points

Point	T,ºC	P,bar	Component	Mole
1	180	8.03	N_2(79%) O_2(21%)	48.75
2	130	8.00	N_2(79%) O_2(21%)	48.75
3	262	15.20	CH_4O(4%) H_2(64%) CO(32%)	4.74
4	223	15.20	N_2(79%) O_2(21%)	48.75
5	600	15.10	Fe_2O_3(100%)	2.00
6	641	15.20	N_2(79%) O_2(21%)	45.34
7	215	15.20	CH_4O(4%) H_2(64%) CO(32%)	1.45
8	425	15.20	FeO(100%)	4.00
9	1000	15.10	N_2(82%) O_2(18%)	43.84
10	1300	15.00	N_2(81%) O_2(13%) CO_2(2%) H_2O(4%)	44.89
11	300	1.03	N_2(81%) O_2(13%) CO_2(2%) H_2O(4%)	35.20
12	588	1.03	N_2(81%) O_2(13%) CO_2(2%) H_2O(4%)	35.20
13	425	15.00	CO_2(33%) H_2O(66%)	3.42

Table 3 Result of exergy analysis

Items	The new system		Chemically intercooled CC	
	Exergy (kJ/mol-CH_4O)	Ratio (%)	Exergy (kJ/mol-CH_4O)	Ratio (%)
Lower heating value	636		636	
Input exergy of fuel (HHV)	676.92	100	676.92	100
Exergy destruction				
HRSG	13.69	2.02	15.51	2.29
Compressor	20.75	3.06	16.22	2.4
Gas turbine	23.60	3.49	18.48	2.73
Combustor	161.05*	23.79	208.1	30.74
Decomposition reaction	6.62	0.98	8.83	1.31
Heat exchanger	24.64	3.64	34.46	5.09
Exhaust gas loss	28.98	4.28	16.59	2.45
Total exergy destruction	279.32	41.26	318.19	47.08
Output exergy (Net power)	387.13	57.19	356.60	52.68
Sum of exergy	675.10	99.88	675.09	99.76
Thermal efficiency	60.60		56.10	

*sum of reduction and oxidation

4   Copyright © 2008 by ASME

The results show that the new system provides a higher efficiency than that of the reference system without CO_2 separation. At the same time, it may separate 70% of the CO_2.

Table 3 shows the exergy destruction in the new system compared to the reference system without CO_2 recovery. The gas turbine inlet temperature of the reference system was set at 1300°C, and the approach temperature difference of the heat exchanger and efficiency of the corresponding assembly are the same as the new system. Obviously, it can be seen that the thermal efficiency of the new system would be expected to be 60.6%, higher than that of the reference system without CO_2 recovery (56.1%). Considering the CO_2 separation, when the reference system separates CO_2 by conventional physical or chemical absorption, its thermal efficiency would be decreased by 6-8 percentage points under the condition of separating about 70% of CO_2, with the same ratio of CO_2 separation as the new system. This indicates that, the new system would be 10-12 percents higher than the reference system with the same ratio of CO_2 separation.

GRAPHICAL EXERGY ANALYSIS OF THE TWO METHANOL GAS TURBINE CYCLES

With the development of complex cycles including complicated chemical/thermal processes, many researchers have paid close attention to the exergy principle for analysis, optimization, and synthesis of the thermal/chemical systems. In order to reveal the internal phenomena of the key processes in the new system, the graphical exergy analysis (EUD methodology), proposed by Ishida [16], was adopted. The EUD (energy-utilization diagram) methodology we used here focuses graphically on the energy level difference in a pair of energy donor and energy acceptor. Both the variation of energy level and energy quantity are graphically shown with $A-\Delta H$ coordinates. Here, the energy level A is a dimensionless criterion ($A=\Delta E/\Delta H=1-T_0\times\Delta S/\Delta H$, a ratio of exergy change to energy change), and the energy quantity ΔH refers to any kind of energy changes, such as thermal energy, power consumption or generation, and energy change in chemical reaction, etc.

The x-coordinate in the EUD is energy change, and the y-coordinate is energy level A. For an energy-transformation process, there exists an energy donor and an energy acceptor, so the exergy destruction is illustrated by the shaded areas between the curves of the energy donor and energy acceptor. In this way, the EUD methodology has particular advantages over conventional exergy methods in showing: (i) the energy level degradation in each process, instead of only magnitudes of exergy losses obtained from the exergy value difference between the output and input of units; (ii) the variation of driving force by dividing the whole process into infinitive processes; (iii) both global and special information on different phenomena such as work, thermal and chemical processes. Hence, the EUD methodology may provide information on the feasibility of process, driving force, defect points, and potential of improvement from intuitive and global viewpoints [17].

Reaction subsystem: For the gas turbine cycle without CLC combustion, the left part of Figure 3a shows the methanol decomposition process. The curves of $A_{ed,1}$ acting as the energy donors, respectively present the energy levels of intercooling heat from the intercooler, while the curve of $A_{ea,decompose}$ represents the energy level of the methanol decomposition acting as the energy acceptor. The shaded area between the curves of the energy donor and energy acceptor represents the exergy destruction in the methanol decomposition, 8.83kJ/mol-CH_4O.
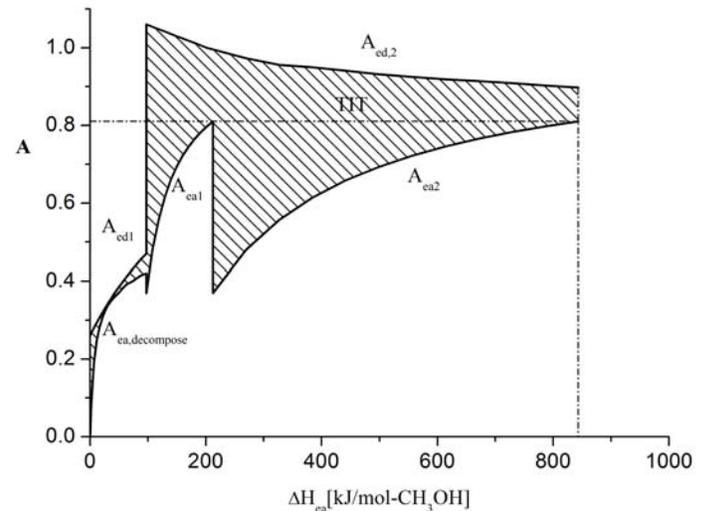
Figure 3a   EUD for combustion of reference system
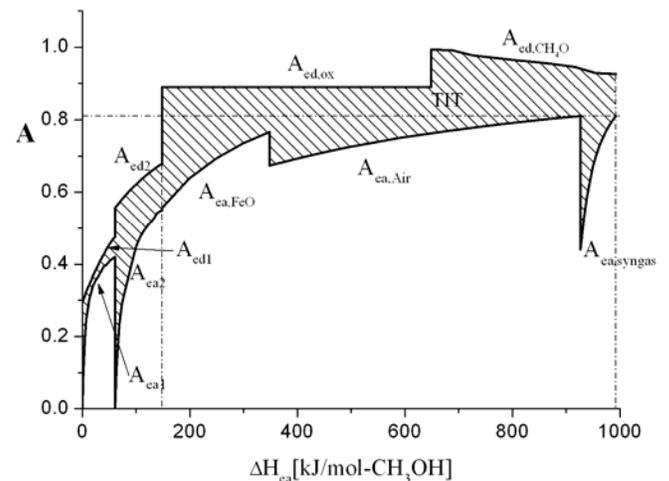
Figure 3b   EUD for reaction of new system

The right part of Figure 3a illustrates that the width of curve $A_{ed,syngas}$ is identical to the heat released by combustion of syngas, and that the heights of the curves indicate the energy level degradation due to transformation of chemical energy into the thermal energy. The heating processes of syngas and combustion air act as the energy acceptor, which are illustrated by the curves of A_{ea1} and A_{ea2}, respectively. The area between

Copyright © 2008 by ASME

A_{ed} and A_{ea} refers to the exergy destruction caused by the syngas combustion with air to the thermal energy at the turbine inlet temperature of 1300°C. Hence, the overall exergy destruction in the combustion of syngas is 208kJ/mol-CH_4O.

In the new gas turbine cycle with CLC, figure 3b shows the four processes in the reaction subsystem.

The first area between A_{ed1} and A_{ea1} shows the methanol decomposition process. The exergy destruction is 6.62kJ/mol-CH_4O, less than that of the reference system (8.83kJ/mol-CH_4O).

The second area of figure 3b represents the reduction of Fe_2O_3 by syngas in which the curve of $A_{ed,2}$ represents the energy level of the Fe_2O_3 acting as the energy donor, with the released thermal energy used to supply the heat of the endothermic reaction. In addition, the energy level of reduction reaction is represented by A_{ea2}. It should be noted that when using syngas-fuelled chemical-looping combustor, the reduction of Fe_2O_3 by syngas is an endothermic reaction. The released heat and exergy destruction in reduction, is 23.50kJ/mol-CH_4O, corresponding to 3.47% based on the input methanol exergy.

The oxidation reaction is shown as the third area of figure 3b and the fourth area is the supplementary combustion process. In the oxidation part, the curves of $A_{ed,ox}$ and $A_{ed,CH4O}$ act as the energy donor. The oxidation takes place at the temperature of 1000°C and at the pressure of 15bar. The heating processes of FeO and combustion air act as the energy acceptor, which are illustrated by the curves of $A_{ea,FeO}$ and $A_{ea,air}$, respectively. The shaded area between the energy donors and energy acceptors represent the exergy destruction in the combustion process. To increase the TIT, a supplementary combustion combustor, which takes place at the temperature of 1300°C, is adopted. As a result, the total exergy destruction of combustion is 137.55kJ/mol-CH_3OH in the new system.

Finally, the overall exergy destruction in the reaction subsystem including the decomposition, reduction and oxidation is 167.67kJ/mol-CH_4O, which is lower than that of the reference system (216.93kJ/mol-CH_4O).

Heat exchanger subsystem: Figure 4a shows the exergy destruction in the dual-pressure heat recovery steam generation and the exergy waste of flue gases. The curve of A_{ed1} represents the energy level of the N_2/O_2 from the turbine acting as energy donor. The minimum temperature difference of 15°C in HRSG is considered. The total exergy destruction in the heat subsystems is 34.46kJ/mol-CH_4O (as shown in Table 3).

Figure 4b illustrates the degradation of energy level in the heat exchange subsystem of new system, where the left area shows the exergy destruction in the recovery of the sensible heat of mid-temperature flue gas and high-temperature Fe_2O_3 particles. The energy level of the solid Fe_2O_3 is represented by the curve A_{ed1}, and the energy level of flue gas is A_{ed2}. The released heat is used to raise the temperature of the pressurized air from the compressor (curve of A_{ea1}). First, the pressurized air is heated to 490°C by flue gae, and then is reheated to 641°C

by Fe_2O_3. The minimum temperature difference between pressurized air (A_{ea1}) and Fe_2O_3 (A_{ed1}) is 120°C and that between pressurized air (A_{ea1}) and flue gas (A_{ed2}) is 100°C. In addition, the right part shows the exergy destruction in the dual-pressure heat recovery steam generation (as shown in area between A_{ed2} and A_{ea2}) and the loss of the flue gases, containing both N_2/O_2 (curve of A_{ed3}) and CO_2 as well as H_2O (curve of A_{ed4}), to the environment (as shown in the two areas on the right side). The total exergy destruction in the heat subsystems is 24.64kJ/mol-CH_4O (as shown in Table 3).
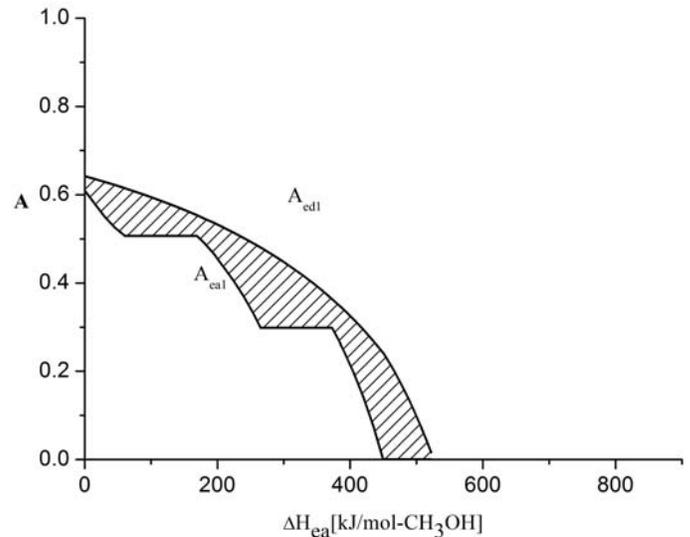
Figure 4a EUD for the heat exchanger subsystem of the reference system
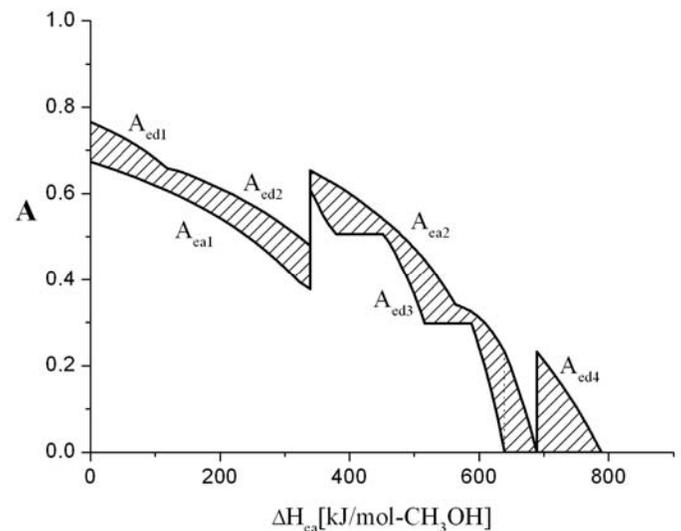
Figure 4b EUD for the heat exchanger subsystem of the new system

6   Copyright © 2008 by ASME
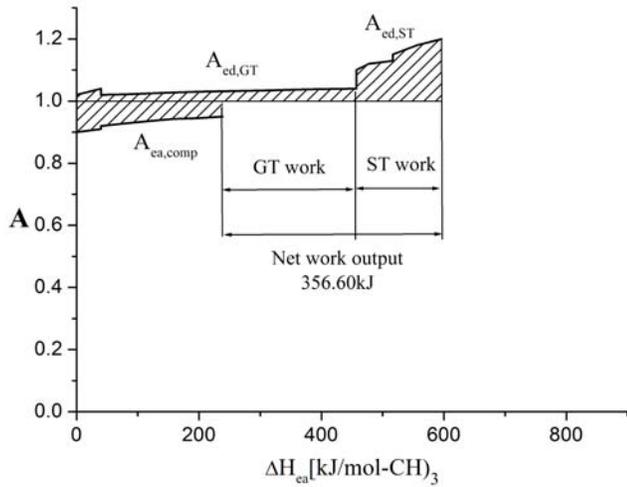
Figure 5a EUD of the power subsystem of the reference system
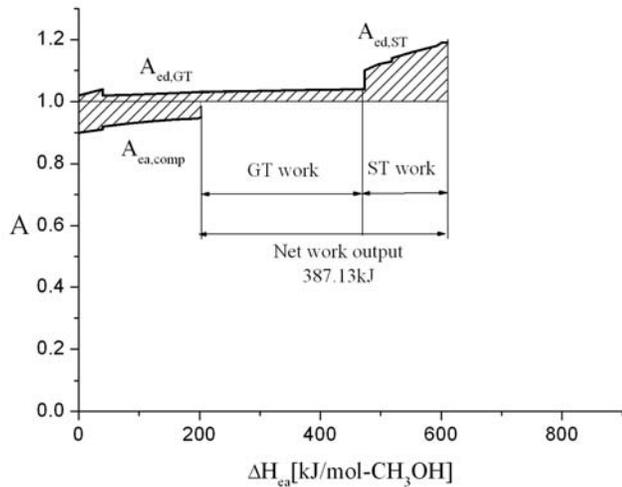
Figure 5b EUD of the power subsystem of the new system

Power subsystem: Figure 5a depicts the exergy destructions in the power subsystem caused mainly by the turbine and power consumption. The exergy destruction in the turbine corresponds to the area between the curve of A_{ed} and A_{ea} in Figure 5a. The total exergy destruction in the power subsystem caused by the turbine (18.48kJ/mol-CH$_4$O) and by the compressor (16.22kJ/mol-CH$_4$O) is 34.70kJ/mol-CH$_4$O. The power output from the turbine is 356.60kJ/mol-CH$_4$O, characterized by a lower output pressure (1.03bar).

Comparatively, the exergy destruction in the turbine and compressor for the new gas turbine cycle is 29.88kJ/mol-CH$_4$O, as shown in Figure 5b, which is caused by the inefficiency of the turbine and compressor. Obviously, we can identify a significant difference of exergy destruction between the two power subsystems. The efficiency of the new cycle at the turbine inlet temperature (TIT) of 1300°C is 60.6% based on the lower heating value (LHV). This new cycle has approximately an 8 percentage point higher efficiency than that of the reference gas turbine cycle using the state of the art technology (TIT=1300°C) with CO_2 separation.

RESULTS AND DISCUSSION

Features of Synergistically Integrating CLC and Methanol Decomposition

Significant decrease of exergy destruction in the combustion. The CLC subsystem is a key process for this new system. We have seen that CLC plays significant role in decreasing the exergy destruction in the new system. To disclose the characteristic of CLC, we examine the interrelationship between the reduction and oxidation reactors.

The CLC combustion is presented in the Figure 6. We assumed that the temperature of the oxidation reaction is constant. The parameters of ΔH and ΔE represent enthalpy and exergy, respectively. First, the oxidation reaction and reduction reaction is at the equilibrium temperature. ΔH_{ox} is the exothermic heat of oxidation and ΔH_{re} is the endothermic heat of reduction at the equilibrium temperature. Since ΔH_{ox} and ΔH_{re} are not affected by the reaction temperature so much, thereby in our study, ΔH_{ox} and ΔH_{re} can be assumed as the constant. Then the temperature of these two reactions reaches the real reaction temperature.

We assume ΔEXL_1 and ΔEXL_2 as the exergy destruction in oxidation and reduction reaction, respectively

Based on the energy and exergy balance:
Oxidation reactor:
$$\Delta H_{f1} = \Delta H_{in1} + \Delta H_{ox} + \Delta H_3 - \Delta H_4 \qquad (1)$$

Where ΔH_{f1} is the enthalpy output of the oxidation reactor, ΔH_{in1} is the enthalpy of air, ΔH_3 is the enthalpy of FeO and ΔH_4 is the enthalpy of Fe$_2$O$_3$.

$$\Delta E_{f1} + \Delta H_3\eta_3 - \Delta H_4\eta_4 = \Delta H_{f1}\eta_1 + \Delta EXL_1 \qquad (2)$$

Where ΔE_{f1} is the exergy of air, and $\Delta H_3\eta_3$ and $\Delta H_4\eta_4$ is the exergy of FeO and Fe$_2$O$_3$ according to the second law of thermodynamics.

Reduction reactor:
$$\Delta H_{f2} = \Delta H_{in2} + \Delta H_{red} - \Delta H_3 + \Delta H_4 \qquad (3)$$

Where ΔH_{f2} is the enthalpy output of the reduction reactor, and ΔH_{in2} is the enthalpy of fuel.

$$\Delta E_{f2} - \Delta H_3\eta_3 + \Delta H_4\eta_4 = \Delta H_{f2}\eta_2 + \Delta EXL_2 \qquad (4)$$

Where ΔE_{f2} is the exergy of fuel.
According to Annex A [18], the exergy destruction ΔEXL_1 and ΔEXL_2 can be shown as:
$$\Delta EXL_1 = \Delta G_1(1 - \eta_1) \qquad (5)$$
$$\Delta EXL_2 = \Delta G_2(1 - \eta_2) \qquad (6)$$

7 Copyright © 2008 by ASME
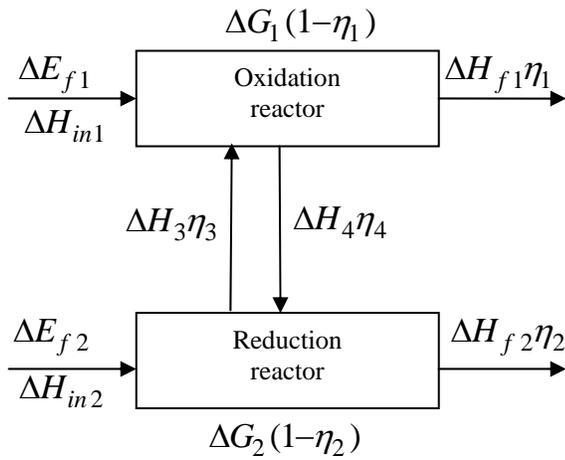
Figure 6 Sketch map of the CLC combustion

Figure 7 Variation in the exergy destruction of the cycle with reduction temperature

The total exergy destruction of the two reactors is:

$$\Delta EXL = \Delta EXL_1 + \Delta EXL_2 = \Delta G_1(1-\eta_1) + \Delta G_2(1-\eta_2) \qquad (7)$$

Introduction of Eq. (2) and Eq. (4) into Eq. (7) becomes

$$\Delta EXL = \Delta E_{f1} + \Delta E_{f2} - \Delta H_{f1}\eta_1 - \Delta H_{f2}\eta_2 \qquad (8)$$

We assume $\Delta H_{ex}=\Delta H_4-\Delta H_3$. So the ΔH_{ex} is the heat exchanged between reduction reactor and oxidation reactor. Introduction of Eq. (1) and Eq. (3) into Eq. (8) becomes

$$\Delta EXL = (\Delta E_{f1} + \Delta E_{f2}) - ((\Delta H_{ox} + \Delta H_{in1})\eta_1 \qquad (9)$$
$$+ (\Delta H_{re} + \Delta H_{in2})\eta_2) + \Delta H_{ex}(\eta_1 - \eta_2)$$

The first item in the right side of Eq. (9) is the exergy input of the CLC system, while the second item is mainly related with the type of metal. The third item shows the effect of ΔH_3 on the system performance. η_2 is a key parameter and depended on the reduction reaction temperature. When the T_{re} decreases, the second and the third items will be increased, thereby reducing the ΔEXL. That is, when the reduction reaction temperature (T_{re}) decreases, the exergy destruction of CLC system is reduced, thereby resulting in better thermodynamic performance of the system.

Eq. (9) can be rearranged as

$$\Delta \eta_{EXL} = \frac{\Delta EXL}{\Delta E_{f1} + \Delta E_{f2}}$$
$$= 1 - \frac{((\Delta H_{ox} + \Delta H_{in1})\eta_1 + (\Delta H_{re} + \Delta H_{in2})\eta_2) + \Delta H_{ex}(\eta_1 - \eta_2)}{\Delta E_{f1} + \Delta E_{f2}} \qquad (10)$$
$$= f(T_{re}, \Delta H_{ex})$$

As a function of T_{re} and ΔH_{ex}, the $\Delta \eta_{EXL}$ will be reduced as the decrease of T_{re} and ΔH_{ex}.

Figure 7 illustrates the overall $\Delta \eta_{EXL}$ of the system as it varies with the reduction reactor temperature and turbine inlet temperature. It can be seen that its exergy destruction is expected to increase 2 percent with the reduction temperature from 400°C to 900°C.

Upgrading of the energy level of low-temperature thermal energy. Another attractive feature is that the low-grade intercooling thermal energy at around 250ºC can be upgraded to the high grade chemical energy of the solid FeO via reduction reaction, and then released as the high-temperature thermal energy via oxidation reaction to produce electricity with a high-efficiency Brayton cycle.

According to the EUDs, it is clear that the low temperature thermal energy from intercooling heat supplies the methanol decomposition, and the reduction reaction absorbs the middle temperature thermal energy from the Fe_2O_3. The intercooling heat is first stored in the syngas through the methanol decomposition, and is then turned into the chemical energy of FeO. The average energy levels of intercooling heat and the heat of Fe_2O_3 is about 0.35 and 0.6, respectively, and the FeO oxidation is about 0.89. Hence, the methanol decomposition process and the reduction reaction raise the energy levels of intercooling heat and the heat from Fe_2O_3.

It should be emphasized that this benefit is attributed to the energy-level degradation from methanol combustion to FeO oxidation in the chemical-looping combustion, meaning that this degradation acts as a "driving force" to upgrade the energy level of low-temperature intercooling thermal energy. The low-temperature intercooling heat is absorbed by the methanol decomposition reaction and the mid-temperature thermal energy of Fe_2O_3 is absorbed by the reduction reaction. The average reaction level A of methanol decomposition is 0.4 (Figure 3b), which is appropriate for absorbing low-temperature thermal energy, and the reduction reaction is 0.5, which is used to absorb mid-temperature thermal energy. The low and mid-temperature energies are finally released as a form of high-temperature thermal energy in the oxidation reactor. It is clear that with the decrease of exergy destruction in the methanol decomposition and reduction reactions, the cascade

8   Copyright © 2008 by ASME

utilization of chemical energy is achieved. This is main benefit from the cascade utilization of energy.

It can be seen from table 3 that in the new cycle the net efficiency could be as high as 60.6%, a competitive figure when compared with that of the current advanced reference system.

Advanced thermodynamic performance

Figure 8 illustrates the variation of the overall thermal efficiency (η) of the system with varying the turbine inlet temperature (TIT) and pressure ratio (π). In addition, for the given π, η will increase with the increase of TIT. For each TIT, there is a π_{opt} to get a maximum of thermal efficiency, which is similar to that of the conventional combined cycle, with the π_{opt} at about 15-17bar. This means that the new system has similar value of π_{opt} with the conventional combined cycle. The thermal efficiency is expected to be about 63.2% at the pressure ratio of 16 at a gas turbine inlet temperature of 1500ºC.
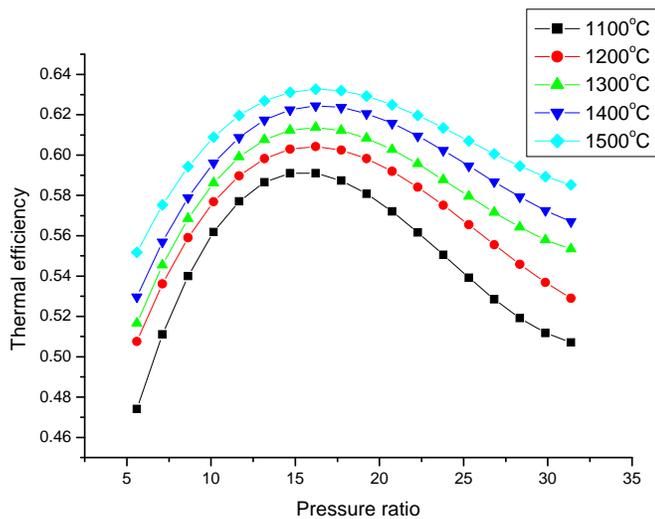
Figure 8   Variation of thermal efficiency with TIT and π

In the reference system, the π_{opt} is about 25-30, which is bigger than the optimize pressure ratio of this new system. It is very difficult to achieve this pressure ratio under the present technology. According to the integration of CLC combustion and methanol decomposition, this new system uses the Fe_2O_3 (stream 5) to reheat the pressured air (stream 3), so that the π_{opt} of the new system is about 15, which is similar to the combined cycle and is easily achievable.

Significant role of decreasing energy penalty for CO_2 capture

In conventional technology for suppressing environmental impact, it can be easily found that the undesirable substances formed from the upstream process are often removed from the downstream process with various separation processes by dealing with a great amount of exhaust gas and at a high cost of energy consumption [19]. The tendency of the next generation systems will be toward the elimination of undesirable formation from the upstream process. From this point, we may find that the CLC combustion will be the promising technology to recover CO_2. Thus, in a thermal cycle with a CLC combustion scenario, environmental pollution due to greenhouse gas emission will be eliminated. Similarly, we may find that the product of the reduction reactor in the chemical-looping combustion is also very simple, consisting of only water and CO_2.

Table 4 illustrates the comparison of CO_2 capture on the three systems (combined cycle, the reference system and the new system) with and without CO_2 compression. The combined cycle is based on MITSUBISHI M701F type, whose turbine inlet temperature is 1350ºC and pressure ratio is 17. If all these three systems remove 70% of CO2, and because of the characteristics of CLC combustion, the thermal efficiency of the new system will not be reduced, but the thermal efficiencies of other two systems will be decreased by about 6 percentages. Considering the transportation, the CO_2 is generally compressed to 85bar to be liquefied and transported. From table 4, it can be seen that the thermal efficiency of the combined cycle and the reference system will be decreased by 1.5 percentages, and the new system will be decreased by 0.8 percentages. This is because the CO_2/H_2 from the reduction reactor is 15bar, a value higher than the exhaust gas of the other systems (1.03bar).

Table 4   Comparison of thermal efficiencies with 70% CO_2 capture

	CC	Reference system	New system
Thermal efficiency (CO_2 without compression)	47.4%	50.3%	60.6%
Thermal efficiency (CO_2 compressed to 85bar)	45.9%	48.8%	59.5%

Considering the CO_2 capture, the new system has an advanced feature without energy penalty, which is 13.6 percentage points higher than the combined cycle, and 10.7 percentage points higher than reference system.

EXPERIMENT OF METHANOL FUELLED AND SYNGAS FUELLED CLC

Chemical-looping combustion is the core technology in the new system. To verify the feasibility of CLC, we have performed several experiments about methanol fuelled and syngas fuelled CLC.

The experiment of the reduction reaction between methanol and Fe_2O_3 was performed.

9   Copyright © 2008 by ASME

The reaction rates of each solid particle were measured by a TGA (thermal gravimetrical analysis) system. The particles were spherical and composed of 60 wt% Fe_2O_3 and 40 wt% Al_2O_3. The preparation method, the dissolution method, was introduced to improve the kinetic characteristics of particles. The particles were prepared by freeze granulation and sintered at 1300^oC for 6h before they were sieved to diameter of 1-2 mm.

For the experiment of reduction, the methanol is evaporated, and then is transferred to the reactor. The reaction temperature is 300^oC. After the Fe_2O_3 is reduced to FeO, the temperature of reactor is heated to 800^oC, and the air is injected into the reactor. The FeO is oxidized to Fe_2O_3.
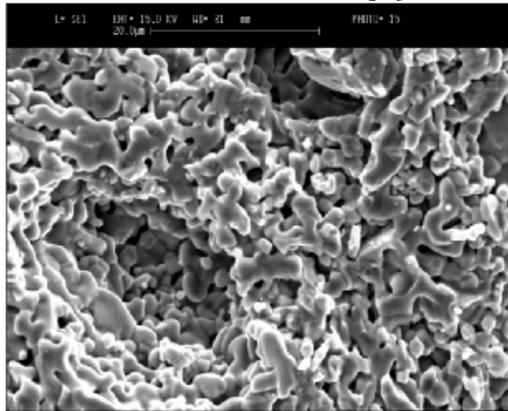
(a) before reaction
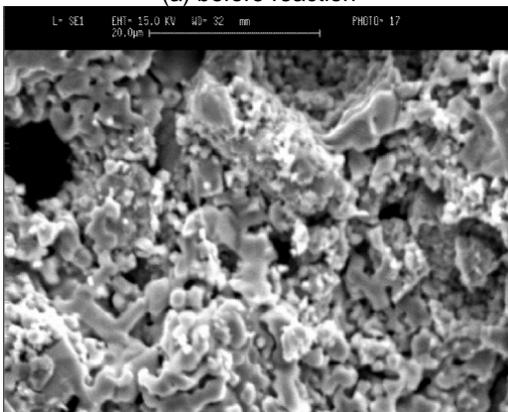
(b) after reaction

Figure 9   Cross-sectional photos of particles

We also have experimentally investigated the kinetics of chemical-looping combustion with simulated syngas in an elevated pressure fixed bed reactor [12]. Two kinds of particles: $NiO/NiAl_2O_4$ and $CoO–NiO/YSZ$ particles were prepared. The particles were shaped in pellet form with 4.0 mm diameter and 1.5 mm in height, and were calcined at 1300^oC for 6 h in the atmosphere. The weight ratio of the solid reactant to the binder was set at 6:4.

By using the SEM (scanning electron microscope), the surface of the particles is investigated. Fig. 9 shows the images of two such particles. This SEM magnifies the particles 2000 times. Before the reaction, the surface of particles is smooth and compact. The surface of particles becomes coarse after reaction. There are many small particles adhering to the big ones, which bring about lots of irregular porosities. These porosities can make the gas diffusing easily, that is helpful for reaction.

An outstanding founding is that syngas is a suitable fuel for chemical-looping combustion. The looping material ($NiO/NiAl_2O_4$) has higher reduction reactivity with syngas. There was no damage to the samples of solid materials, after more than 10 cycles of reduction and oxidation. The syngas fuelled chemical-looping combusting has high reactivity, avoidance of carbon deposition and regenerability.

Furthermore, the reactivity of syngas with Fe_2O_3 will be investigated in more detail to develop the chemical-looping combustion and to promote this new power generation system.

CONCLUSIONS

A novel combined cycle based on the integration of methanol decomposition and chemical-looping combustion (CLC) has been proposed and evaluated by means of graphical exergy methodology. The system study on two methanol-fuelled power plants points out the defects and potential for improvement of the chemically intercooled combined cycle. In the new system, because of integration of the methanol decomposition and CLC combustion, the exergy destruction in combustion process is decreased, the low-temperature intercooling energy is upgraded and the CO_2 is captured without energy penalty. We have clarified that in the new gas turbine cycle with chemical-looping combustion the exergy losses in combustion and power consumption are much lower than in the reference system. As a result, thermal efficiency in this new cycle with current-technology gas turbines (with a turbine inlet temperature of 1300^oC) could be as high as 60.6% with 70% CO_2 recovery, increasing efficiency by at least 8 percentage-points higher efficiency compared to that of the reference system with CO_2 capture. This new gas turbine cycle with methanol-fuelled chemical-looping combustion makes breakthrough in both the efficient use of methanol energy and the mitigation of greenhouse gas impact, and can be expected to be a new-generation power plant.

ACKNOWLEDGMENTS

REFERENCES

[1]   Abu-Khader Mazen M., 2006, "Recent Progress in CO_2 Capture/Sequestration: A Review", Energy Sources, Part A: Recovery, Utilization, and Environmental Effects, Vol. 28(14), pp. 1261 - 1279

Copyright © 2008 by ASME

[2] Assistant Secretary for Fossil Energy, 1993, "Clean Coal Technology Demonstration Program", Report of DOE/ASME, U.S. DOE

[3] Gottlicher G., Pruschek R., 1997, "Comparison of CO_2 Removal Systems for Fossil-fuelled Power Plant Processes". Energy Convers Mgmt, 38(suppl.), 173

[4] Ishida M., Jin H., 1994, "A New Advanced Power-Generation System Using Chemical-looping Combustion." Energy, Vol. 19(4), 415

[5] Ishida M., Jin H., 1995, Chemical Looping Combustion Power Generation Plant System. United States Patent, No. 5447024.

[6] Anheden M., 1997, "Analysis of Chemical-looping Combustion Systems for Power Generation", Technical Licentiate Thesis, Royal Institute of Technology, Dept. of Chem. Eng. & Tech., Energy Processes, [ISSN 1104-3466, ISRN KTH/KET/R–62–SE]

[7] Consonni S., Lozza G., Pelliccia G., Rossini S., Saviano F., 2006, "Chemical-Looping Combustion for Combined Cycles with CO_2 Capture", J Eng Gas Turb Power, Vol. 128, pp. 525-534

[8] Mattisson T., Lyngfelt A., 2001, "Application of Chemical-looping Combustion with Capture of CO_2", the 2nd Nordic Mini-Symposium on Carbon Dioxide Capture and Storage. Göteborg, Sweden

[9] Lee J. B., Prak C. S., Choi S., Song Y. W., 2005, "Redox Characteristics of Various Kinds of Oxyen Carriers for Hydrogen Fueled Chemical-looping Combustion", Journal of Industrial and Engineering Chemistry, Vol. 11(1), pp. 96-102

[10] Copeland RJ., Alptekin G., Cesario M., Gebhard S., Gershanovich Y., 2001, "A Novel CO_2 Separation System", Report of United States Department, DOE

[11] Jin H., Ishida M, 2000, "A Novel Gas Turbine Cycle with Hydrogen-fueled Chemical-looping Combustion", Int J of Hydrogen Energy, Vol. 25(12), pp. 1209-1215

[12] Jin H., Ishida M., 2004, "A New Type of Coal Gas Fueled Chemical-looping Combustion", Fuel, Vol. 83(17-18), pp. 2411-2417

[13] Jin H., Okamoto T., Ishida M., 1999, "Development of a Novel Chemical Looping Combustion: Synthesis of a Solid Looping Material of $NiO/NiAl_2O_4$", Ind. Eng. Chem. Res., Vol. 38 (1), pp. 126 -132

[14] Jin H., Okamoto T., Ishida M., 1998, "Development of a Novel Chemical-looping Combustion: Synthesis of a Looping Material with a Double Metal Oxide of CoO-NiO", Energy Fuels, Vol. 12 (6), pp. 1272 -1277

[15] Jin H., Hong H., Cai R., 2006, "A Chemically Intercooled Gas Turbine Cycle for Recovery of Low-Temperature Thermal Energy", Energy, Vol. 31, pp. 1554-1566

[16] Ishida M., Kawamura K., 1982, "Energy and Exergy Analysis of a Chemical Process System with Distributed Parameters Based on the Energy-Direction Factor Diagram", Industrial Engineering and Chemistry Process Design & Development, Vol. 21, pp. 690-695

[17] Jin H., Ishida M., 1994, "Graphical Exergy Analysis of a New Type of Advanced Cycle with Saturated Air", Heat Recovery Systems and CHP, Vol. 14, Issue 2, pp 105-116

[18] Jin H., Hong H., Wang B., Han W., and Lin R., 2005, "A New Principle of Synthetic Cascade Utilization of Chemical Energy and Physical Energy," J. Science in China Ser. E Engineering & Material Science (In English), Vol. 48(2), pp. 163-179

[19] Riemer P., 1996, "Greenhouse Gas Mitigation Technologies, an Overview of the CO_2 Capture, Storage, and Future Activities of the IEA Greenhouse Gas R&D Program," Energy Convers. Mgmt, Vol. 37(6-8), pp. 665-670

Based on the general functions of Gibbs free energy and exergy, Gibbs free energy change dG and exergy change dE in a process of chemical reaction, at a given temperature T and under a pressure p, are, respectively, given as:

$$dG = dH - TdS \qquad (1)$$
$$dE = dH - T_0 dS \qquad (2)$$

where dH (kJ/mol) is the total enthalpy change in a process, TdS (kJ/mol) is the heat-equivalent energy in a process, and dS (kJ/K.mol) is the entropy change in a process, T refers to reaction temperature (K) and T_0 denotes the environment temperature (K).

For the energy conversion and utilization in a combustion process, Gibbs free energy ΔG in a combustion reaction cannot produce the work, and the total enthalpy change ΔH_f is completely transformed into thermal energy. For simplicity, we assumed that a combustion process might be divided into two sections: an exothermic reaction at a given high temperature T and a heat transfer process within the working substance of thermal cycle. Based on Eq. (1) and Eq. (2), exergy of fuel ΔE_f and Gibbs free energy change ΔG are, respectively, obtained:

$$\Delta G = \Delta H_f - T\Delta S \qquad (3)$$

$$\Delta E_f = \Delta H_f - T_0\Delta S \qquad (4)$$

and then, the entropy change ΔS may be given by Eq. (3)

$$\Delta S = \frac{\Delta H_f - \Delta G}{T} \qquad (5)$$

Introduction of Eq. (3) into Eq. (4) yields

$$\Delta E_f = \Delta H_f(1-\frac{T_0}{T}) + \Delta G\frac{T_0}{T} \qquad (6)$$

Since $T_0/T = 1-(1-T_0/T)=1-\eta_c$, Equation (6) may be reduced to：

$$\Delta E_f = \Delta H_f\eta_c + \Delta G(1-\eta_c) \qquad (7)$$

Equation (7) states that the exergy of fuel in combustion (ΔE_f) is composed of two parts: work-equivalent energy of $\Delta G(1-\eta_c)$, associated with chemical exergy, and thermal exergy of $\Delta H_f\eta_c$. Traditionally, $\Delta G(1-\eta_c)$ is often regarded as a exergy destruction in the combustion reaction. It is also found from exergy balance that ΔE_f represents the exergy input, $\Delta H_f\eta_c$ refers to the thermal exergy output, and correspondingly $\Delta G(1-\eta_c)$ stands for the exergy destruction. On the other hand, an important thing we emphasized here is that a part of $\Delta G(1-\eta_c)$ should be taken into account as an usable chemical exergy which is not simply destroyed as a form of destruction. Hence, Equation (7) indicates the interrelationships between exergy of fuel ΔE_f and Gibbs free energy in combustion reaction, and more important, it reveals that the effective use of chemical exergy $\Delta G(1-\eta_c)$ is a key point of reducing exergy destruction in combustion of fuel.

Copyright © 2008 by ASME